REPORT DOCUMENTATION PAGE

Form Approved OMB No. 0704-0188

1. REPORT DATE *(DD-MM-YYYY)*	2. REPORT TYPE	3. DATES COVERED *(From – To)*
22-09-2008	Final Report	1 September 2007 – 31 August 2008

4. TITLE AND SUBTITLE

Unsteady Aerodynamics of Membrane Airfoils

5a. CONTRACT NUMBER
FA8655-07-1-3044

5b. GRANT NUMBER
Grant 07-3044

5c. PROGRAM ELEMENT NUMBER
61102F

6. AUTHOR(S)

Professor Ismet Gursul

5d. PROJECT NUMBER

5d. TASK NUMBER

5e. WORK UNIT NUMBER

7. PERFORMING ORGANIZATION NAME(S) AND ADDRESS(ES)
University of Bath
Claverton Down
Bath BA2 7AY
United Kingdom

8. PERFORMING ORGANIZATION REPORT NUMBER

9. SPONSORING/MONITORING AGENCY NAME(S) AND ADDRESS(ES)

EOARD
Unit 4515 BOX 14
APO AE 09421

10. SPONSOR/MONITOR'S ACRONYM(S)

11. SPONSOR/MONITOR'S REPORT NUMBER(S)
Grant 07-3044

12. DISTRIBUTION/AVAILABILITY STATEMENT

Approved for public release; distribution is unlimited.

13. SUPPLEMENTARY NOTES

14. ABSTRACT

In the first six month of the project, various experimental methods were used to study the unsteady aerodynamics of membrane airfoils. These methods include: measurements of membrane shape with a high speed camera, flow visualization, and Particle Image Velocimetry (PIV) measurements with a high frame rate system. Vibrations of the membrane, mode shapes, frequency were investigated together with velocity measurements at different angles of attack and free-stream velocities. These measurements provide benchmark data for computational simulations carried out by AFRL's Computational Sciences Branch, Air Vehicles Directorate.

In the last six months of this effort, various experimental methods were used to study the unsteady aerodynamics of 2D and 3D membrane wings. These methods include: measurements of membrane shape with high speed cameras, flow visualization, and Particle Image Velocimetry (PIV) measurements with a high frame rate system. Both a two-dimensional airfoil and a finite wing (rectangular wing with aspect ratio AR=2) were investigated. Effects of membrane pre-strain and excess length were studied with emphasis on the unsteady aspects of the fluid-structure interactions. Vibrations of the membrane, mode shapes, frequency were investigated together with velocity measurements at different angles of attack and free-stream velocities. These measurements provide benchmark data for computational simulations carried out by AFRL's Computational Sciences Branch, Air Vehicles Directorate.

15. SUBJECT TERMS
EOARD, Unsteady Aerodynamics, Fluid Dynamics, Micro Air Vehicle

16. SECURITY CLASSIFICATION OF: a. REPORT	b. ABSTRACT	c. THIS PAGE	17. LIMITATION OF ABSTRACT	18, NUMBER OF PAGES	19a. NAME OF RESPONSIBLE PERSON	19b. TELEPHONE NUMBER *(Include area code)*
UNCLAS	UNCLAS	UNCLAS	UL	17	SURYA SURAMPUDI	+44 (0)1895 616021

UNSTEADY AERODYNAMICS OF MEMBRANE AIRFOILS

Contract No: FA8655-07-1-3044

Progress Report for Months 1-6

submitted to

Dr. Surya Surampudi
European Office of Aerospace Research & Development (EOARD)
Bldg 186, Room 31
86 Blenheim Crescent
Ruislip, Middlesex HA4 7HB
United Kingdom

by

Professor Ismet Gursul
Department of Mechanical Engineering
University of Bath
Bath, BA2 7AY
United Kingdom

February 2008

1. SUMMARY

In the first six month of the project, various experimental methods were used to study the unsteady aerodynamics of membrane airfoils. These methods include: measurements of membrane shape with a high speed camera, flow visualization, and Particle Image Velocimetry (PIV) measurements with a high frame rate system. Vibrations of the membrane, mode shapes, frequency were investigated together with velocity measurements at different angles of attack and free-stream velocities. These measurements provide benchmark data for computational simulations carried out by Dr. Ray Gordnier and Dr. Miguel Visbal, Computational Sciences Branch, Air Vehicles Directorate.

2. MAIN FINDINGS

2.1. Wind tunnel experiments

The wind tunnel model, its dimensions and geometry, Reynolds number, and material properties of the membrane used were given in the attached AIAA paper. All the experiments were conducted for zero pre-tension case. The setup produces a nominally two-dimensional flow and also two-dimensional deformation.

2.2. Membrane shape

Figure 1 shows an example of the instantaneous membrane shape obtained by laser sheet visualization and a high speed camera. The images were digitized by MatLab (Image Processing Toolbox) to find the coordinates. From the instantaneous coordinates of the membrane, the time-average membrane shape was calculated for each case. Figure 2 shows the maximum camber as a function of angle of attack at different free stream velocities.

2.3. Mean flow

Figure 3 shows the magnitude of the time-averaged velocity together with streamline patterns at different angles of attack for U_∞=5 m/s. Measurements were taken only for separated flows for which membrane oscillations were observed. At small incidences such as α=12°, there are weakly separated flows and the shear layer stays close to the membrane surface. With increasing angle of attack, the shear layer moves away from the surface.

2.4. Membrane oscillations

Figure 4 shows examples of the variation of the standard deviation of the membrane displacements. For these examples, the second mode of vibrations is identified. Figure 5 shows the mode number and Strouhal number of the membrane oscillations as a function of incidence. At smaller incidences there are mode jumps, and the mode number increases with the free stream velocity. At large incidences, the second mode is observed regardless of the free stream velocity. The variation of the Strouhal number suggests that there might be a coupling of the membrane oscillations with vortex shedding frequency in the wake.

2.5. Unsteady flow

Figure 6 shows the turbulence intensity at different angles of attack. Variation of the Reynolds stress is qualitatively similar. The shear layer fluctuations move away from the surface with increasing angle of attack. The largest membrane oscillations are observed when the shear layer is closest to the surface (α=12°). Peak magnitudes of the fluctuations are observed for α=14° to 18°, then the peak value decreases at higher angles of attack.

2.6. Flow-membrane coupling

Figure 7 shows the variation of the location of the shear layer and membrane displacement as a function of time for α=13° and U_∞=5 m/s. It is seen that the location of the shear layer is highly correlated to the membrane oscillations.

2.7. Comparison of rigid and flexible membranes

A rigid membrane airfoil was manufactured from 1 mm thick stainless steel and tested in order to compare with the flexible membrane airfoil. The profile of the rigid membrane matches that of the average (over incidences) shape of the membrane wing at 5 m/s free stream velocity and at angles of attack from 10 to 18 degrees. Figure 8 shows smoke visualization for the rigid and flexible membrane at α=14°. Figure 9 shows the comparison of the Reynolds stress for the rigid and flexible airfoil at α=18°. It is seen that membrane vibrations excite the shear layer, resulting in the deflection of the shear later towards the membrane. As the separated region is smaller, the drag is likely to be smaller. Hence, this might be a passive method for stall delay.

3. ONGOING WORK

- Membrane shape measurements for nonzero pre-tension cases as well as for excess length;
- PIV measurements for nonzero pre-tension cases as well as for excess length;
- Preliminary design and testing of 3D membrane wings.

APPENDIX

Rojratsirikul, P., Wang, Z., and Gursul, I., "Unsteady Aerodynamics of Membrane Airfoils", (Invited Paper) AIAA-2008-0613, 46th AIAA Aerospace Sciences Meeting and Exhibit, 7-10 January 2008, Reno, NV.

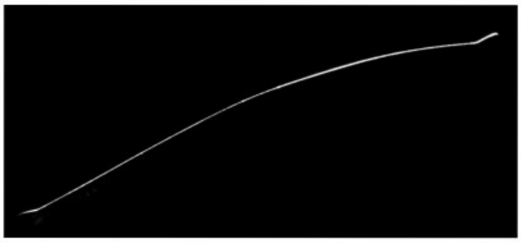

Figure 1: Membrane shape obtained from laser sheet visualization, U_∞=5 m/s, α=20°.

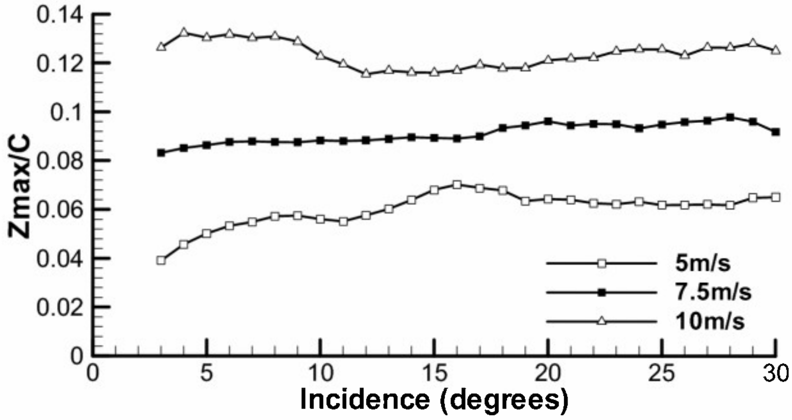

Figure 2: Variation of maximum camber as a function of angle of attack.

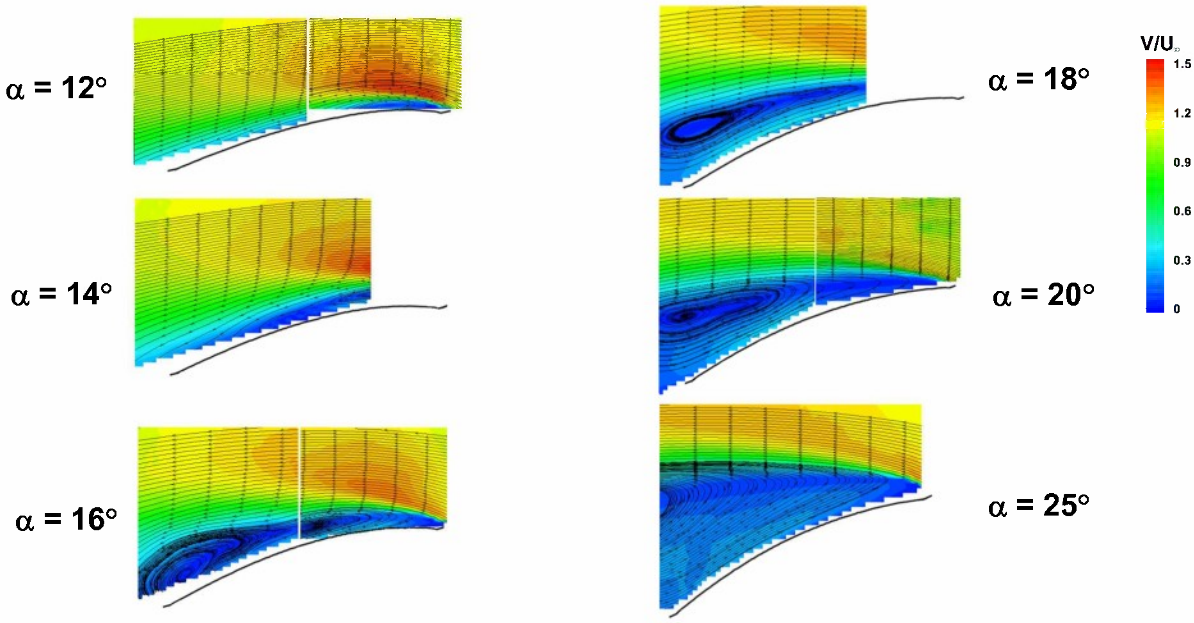

Figure 3: Magnitude of time-averaged velocity and streamlines, U_∞=5 m/s.

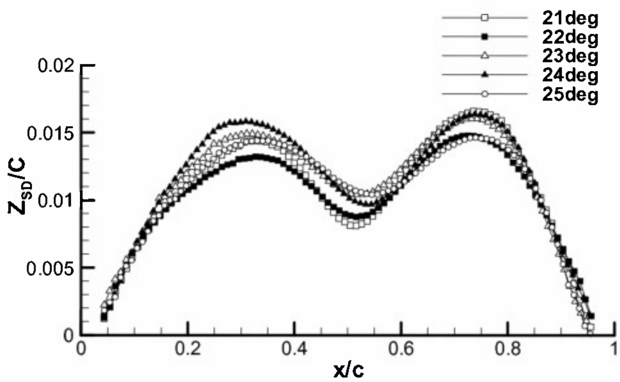

Figure 4: Variation of the standard deviation of the membrane displacement, U_∞=10 m/s.

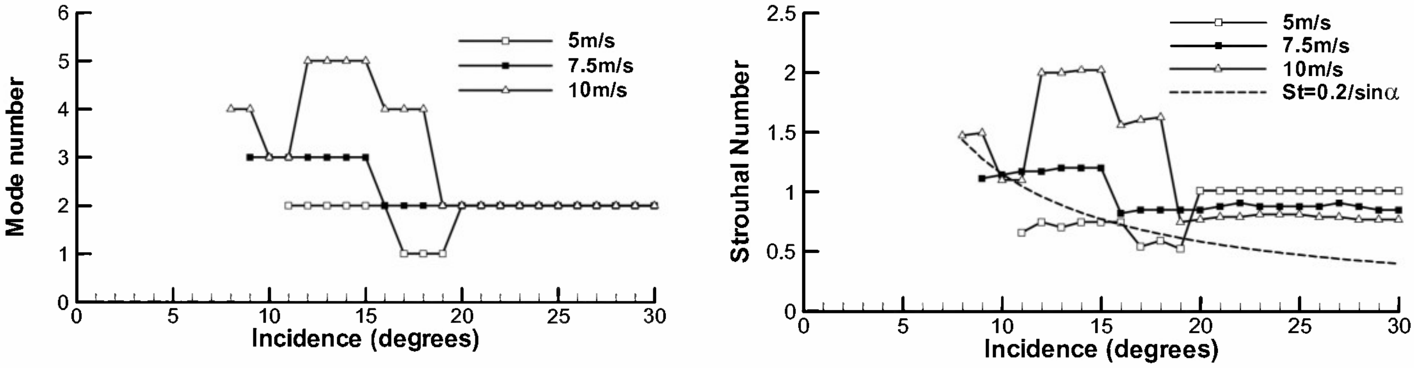

Figure 5: Variation of the mode number (left) and Strouhal number (right) as a function of incidence.

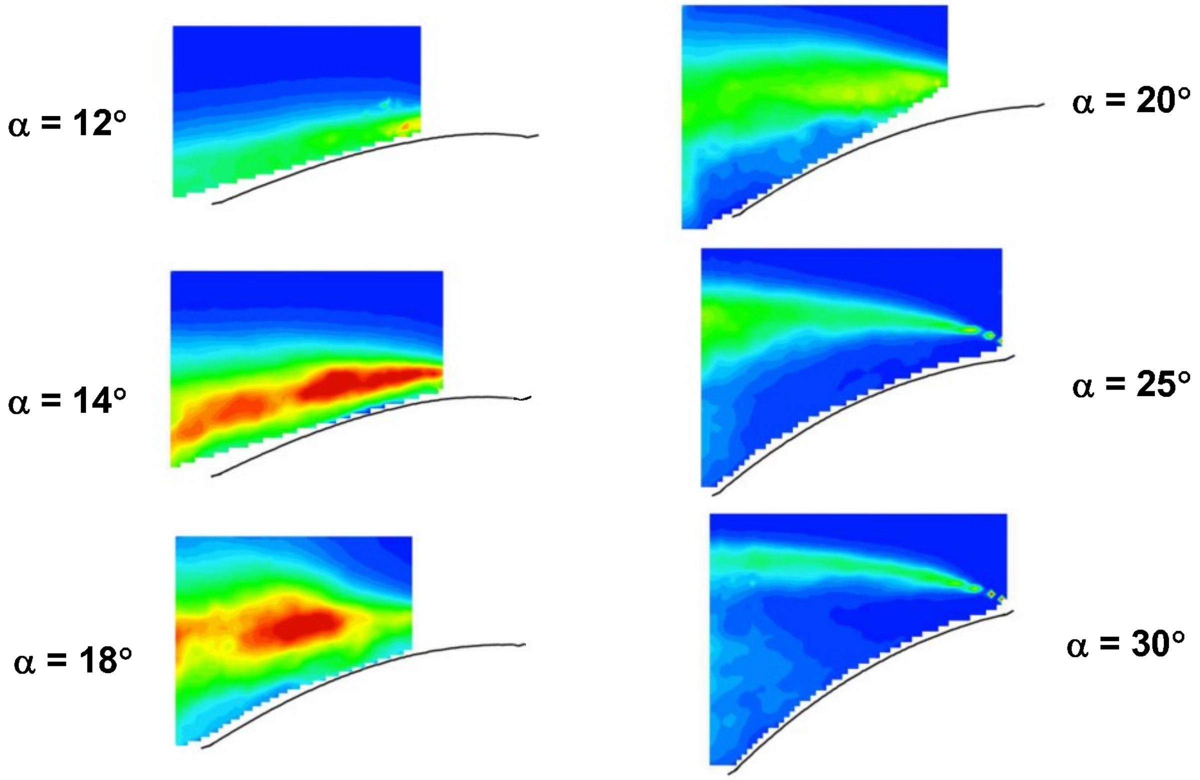

Figure 6: Turbulence intensity at different angles of attack, U_∞=5 m/s.

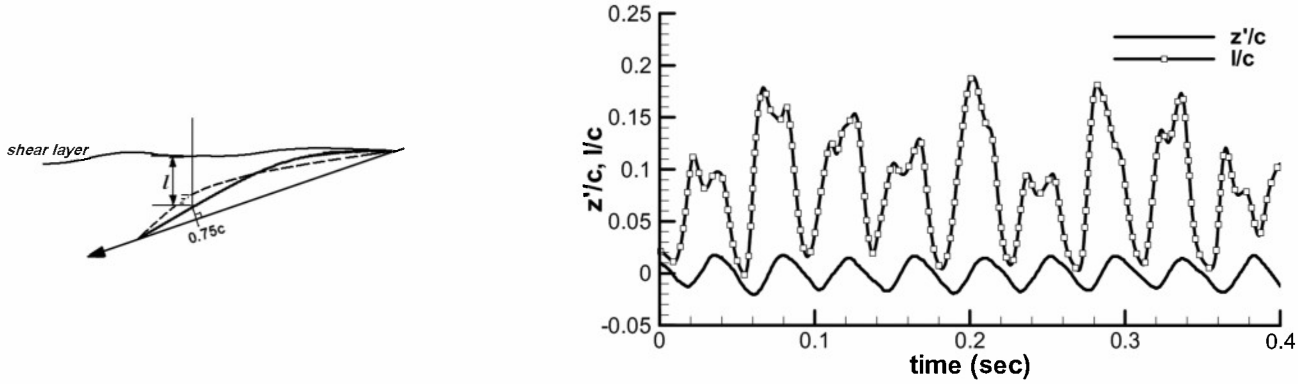

Figure 7: Time history of the location of the shear layer and membrane as measured at 0.75c (see the inset).

$\alpha = 14°$

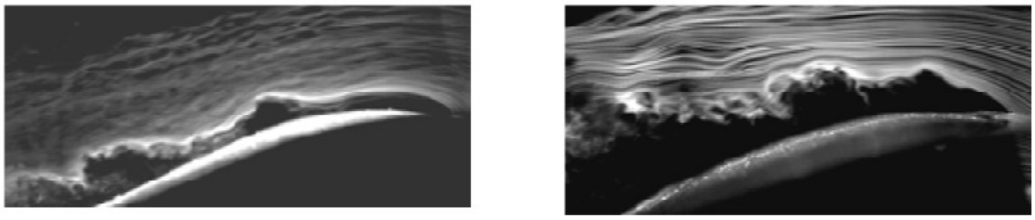

Figure 8: Smoke flow visualization for flexible (left) and rigid (right) membrane, U_∞=5 m/s.

$\alpha = 18°$

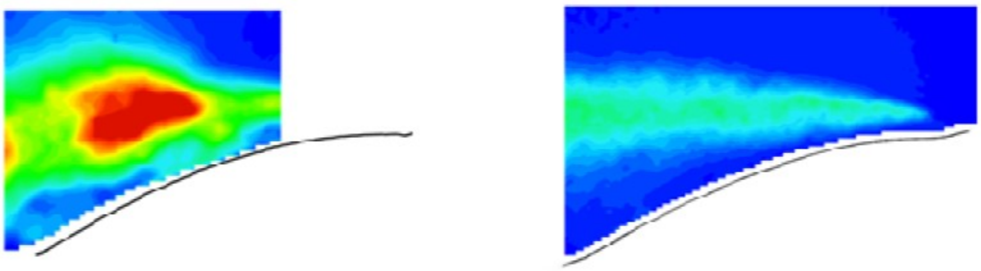

Figure 9: Reynolds stress for flexible (left) and rigid (right) membrane, U_∞=5 m/s.

UNSTEADY AERODYNAMICS OF MEMBRANE AIRFOILS

Contract No: FA8655-07-1-3044

Progress Report for Months 7-12

submitted to

Dr. Surya Surampudi
European Office of Aerospace Research & Development (EOARD)
Bldg 186, Room 31
86 Blenheim Crescent
Ruislip, Middlesex HA4 7HB
United Kingdom

by

Professor Ismet Gursul
Department of Mechanical Engineering
University of Bath
Bath, BA2 7AY
United Kingdom

August 2008

1. SUMMARY

Various experimental methods were used to study the unsteady aerodynamics of 2D and 3D membrane wings. These methods include: measurements of membrane shape with high speed cameras, flow visualization, and Particle Image Velocimetry (PIV) measurements with a high frame rate system. Both a two-dimensional airfoil and a finite wing (rectangular wing with aspect ratio AR=2) were investigated. Effects of membrane pre-strain and excess length were studied with emphasis on the unsteady aspects of the fluid-structure interactions. Vibrations of the membrane, mode shapes, frequency were investigated together with velocity measurements at different angles of attack and free-stream velocities. These measurements provide benchmark data for computational simulations carried out by Dr. Ray Gordnier and Dr. Miguel Visbal, Computational Sciences Branch, Air Vehicles Directorate.

2. MAIN FINDINGS

2.1. Two-dimensional airfoil

The wind tunnel model, its dimensions and geometry, Reynolds number, and material properties of the membrane used were given in the AIAA paper (AIAA-2008-0613). Initially, experiments were conducted for zero pre-tension case. Then, the effects of pre-strain and excess length were investigated. The setup produces a nominally two-dimensional flow and also two-dimensional deformation.

2.2. Membrane shape

Figure 1 shows an example of the instantaneous membrane shape obtained by laser sheet visualization and a high speed camera. The images were digitized by MatLab (Image Processing Toolbox) to find the coordinates. From the instantaneous coordinates of the membrane, the mean and standard deviation of deformation were calculated for each case.

2.3. Membrane vibrations

Figure 2 shows examples of the variation of the standard deviation of the membrane displacements. For these examples, the second mode of vibrations is identified. Figure 3 shows the mode number and Strouhal number of the membrane oscillations as a function of incidence. At smaller incidences there are mode jumps, and the mode number increases with the free stream velocity. At large incidences, the second mode is observed regardless of the free stream velocity. The variation of the Strouhal number suggests that there might be a coupling of the membrane oscillations with vortex shedding frequency in the wake.

2.4. Velocity measurements

The magnitude of the time-averaged velocity together with streamline patterns at different angles of attack are shown in the AIAA paper. Measurements were taken only for separated flows for which membrane oscillations were observed. At small incidences such as α=12°, there are weakly separated flows and the shear layer stays close to the membrane surface. With increasing angle of attack, the shear layer moves away from the surface.

Figure 4 shows the turbulence intensity at different angles of attack. Variation of the Reynolds stress is qualitatively similar. The shear layer fluctuations move away from the surface with increasing angle of attack. The largest membrane oscillations are observed when the shear layer is closest to the surface (α=12°). Peak magnitudes of the fluctuations are observed for α=14° to 18°, then the peak value decreases at higher angles of attack.

2.5. Comparison of rigid and flexible membranes

A rigid membrane airfoil was manufactured from 1 mm thick stainless steel and tested in order to compare with the flexible membrane airfoil. The profile of the rigid membrane matches that of the average shape of the membrane wing at 5 m/s free stream velocity. Figure 5 shows smoke visualization for the rigid and flexible membrane at α=14°. It is seen that membrane vibrations excite the shear layer, resulting in the deflection of the shear later towards the membrane. As the separated region is smaller, the drag is likely to be smaller. Hence, this might be a passive method for stall delay.

2.6. Effect of pre-strain and excess length

Figure 6 shows the variation of the maximum camber as a function of incidence for different pre-strains (δ_0 = 0, 2.5%, and 5%) and excess-length (ε = 2.5% and 5%) for U_∞ = 7.5 m/s. Figure 7 shows the mode number of the membrane oscillations as a function of incidence. It is seen that wings with excess-length exhibit higher modes. Corresponding Strouhal numbers, fc/U_∞, are shown in Figure 8. At relatively high angles of attack, the Strouhal number has similar values regardless of the wing's pre-strain and excess length. However, at smaller incidences there are large differences in the vibration frequency.

Figure 9 shows that membrane wings with excess-length exhibit earlier roll-up of the vortices and smaller separated flow regions, whereas the membranes with pre-strain generally behave more similar to a rigid wing.

2.7. Rectangular wing

An aspect ratio AR=2 rectangular wing was tested. Membrane was fixed at all edges to a metal frame. Two high speed cameras were used in a Digital Image Correlation (DIC) system. Mean and standard deviation of the deformation are shown in Figure 10 for $U_\infty = 5$ m/s and $\alpha = 10°$. At the mid-span plane, the mode number of the vibrations is three. Near the tips, unsteady membrane oscillations are clearly seen. Further analysis of the deformation data is ongoing.

2.8. Other wings

Experiments with a delta wing ($\Lambda = 50°$) with membrane fixed all around the edges were also preformed. Currently, the data are being analyzed.

2.9. Unsteady pitching membrane wing

In order to simulate a gust encounter, a rectangular membrane wing was subjected to a sinusoidal pitching motion. Unsteady deformation data were captured and being analyzed at the moment. The results will be presented in a future publication.

PUBLICATIONS

[1] Rojratsirikul, P., Wang, Z., and Gursul, I., "Unsteady Aerodynamics of Membrane Airfoils", (Invited Paper) AIAA-2008-0613, 46th AIAA Aerospace Sciences Meeting and Exhibit, 7-10 January 2008, Reno, NV.

[2] Rojratsirikul, P., Wang, Z., and Gursul, I., "Unsteady Fluid-Structure Interactions of Membrane Airfoils at Low Reynolds Numbers", submitted to the *Experiments in Fluids*.

[3] Rojratsirikul, P., Wang, Z., and Gursul, I., “Effect of Pre-strain and Excess Length on Unsteady Fluid-Structure Interactions of Membrane Airfoils”, accepted to the AIAA conference in January 2009.

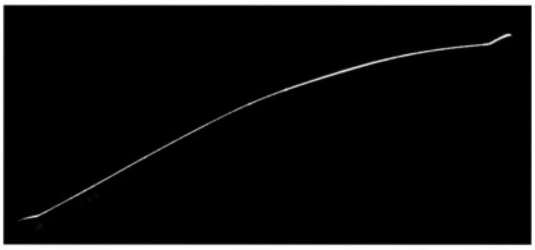

Figure 1: Membrane shape obtained from laser sheet visualization, U_∞=5 m/s, α=20°.

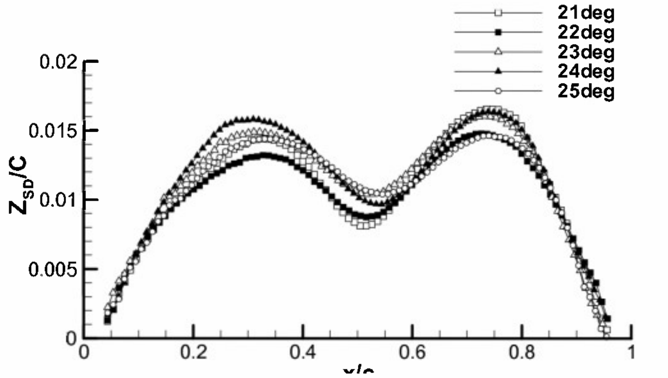

Figure 2: Variation of the standard deviation of the membrane displacement, U_∞=10 m/s.

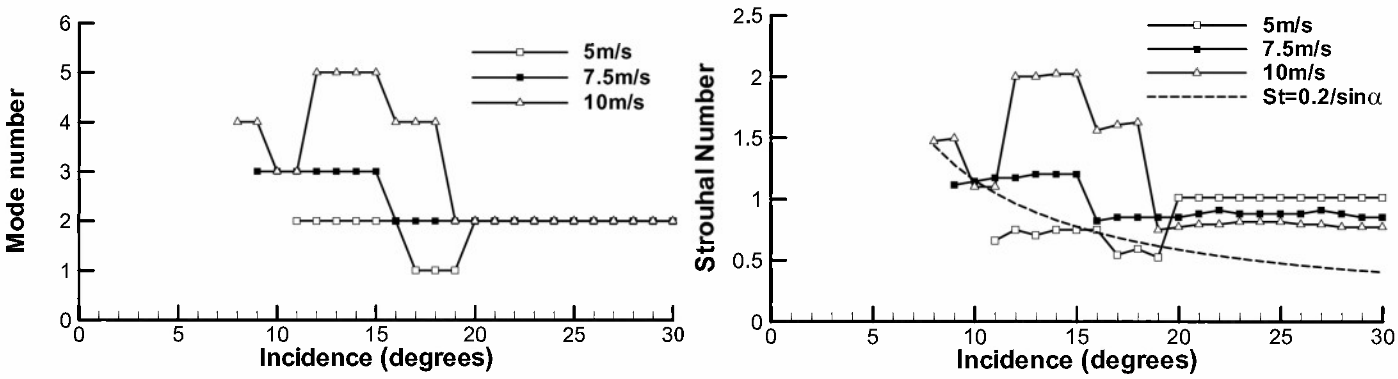

Figure 3: Variation of the mode number (left) and Strouhal number (right) as a function of incidence.

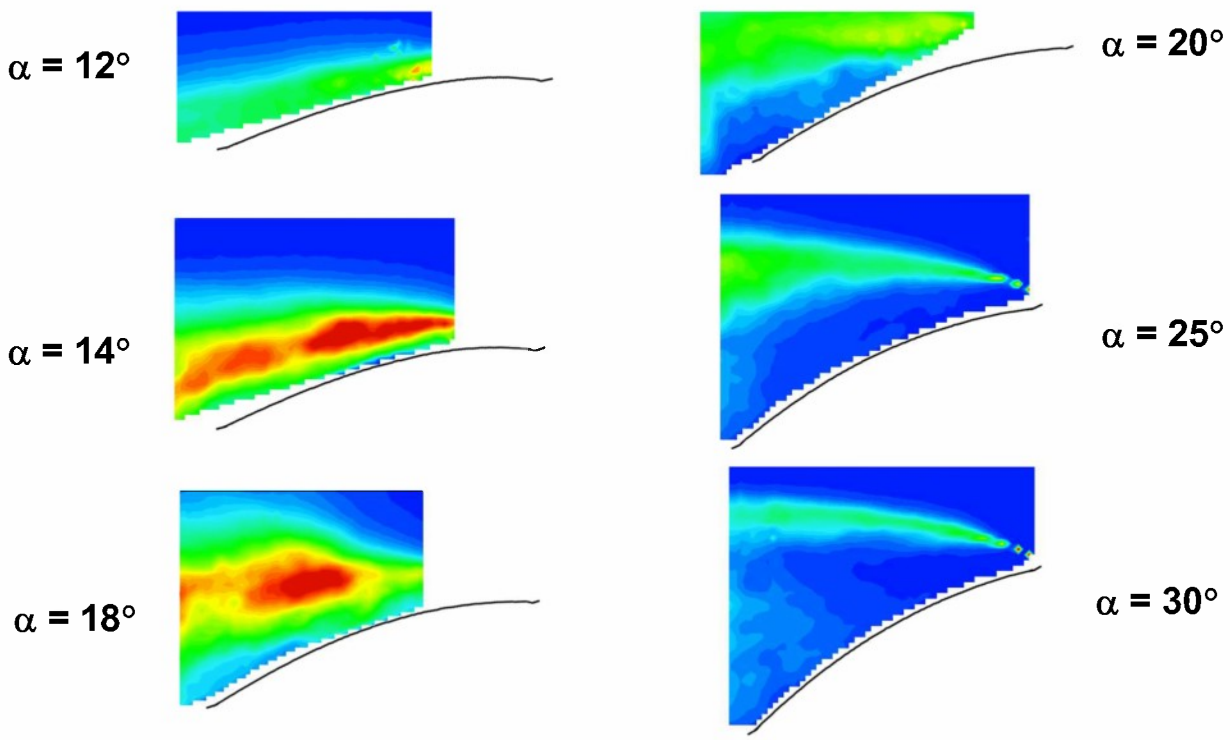

Figure 4: Turbulence intensity at different angles of attack, U_∞=5 m/s.

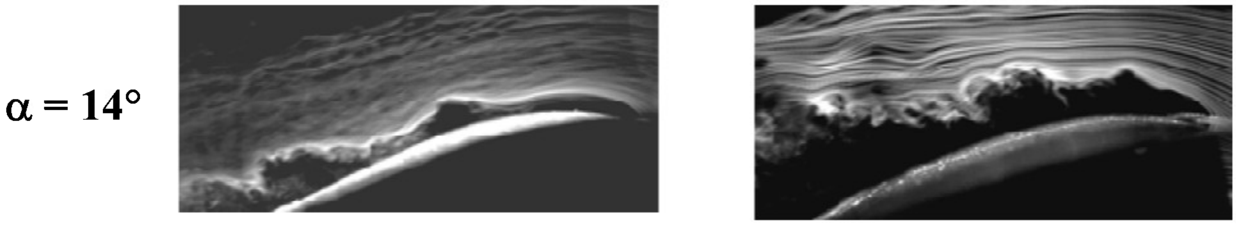

Figure 5: Smoke flow visualization for flexible (left) and rigid (right) membrane, U_∞=5 m/s.

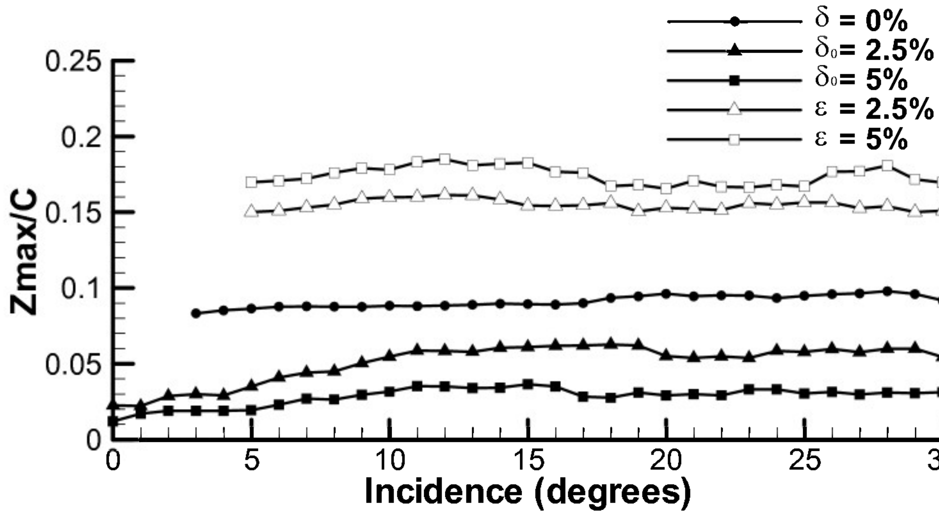

Figure 6: Variation of maximum camber as a function of incidence for different pre-strains and excess lengths , U_∞= 7.5 m/s

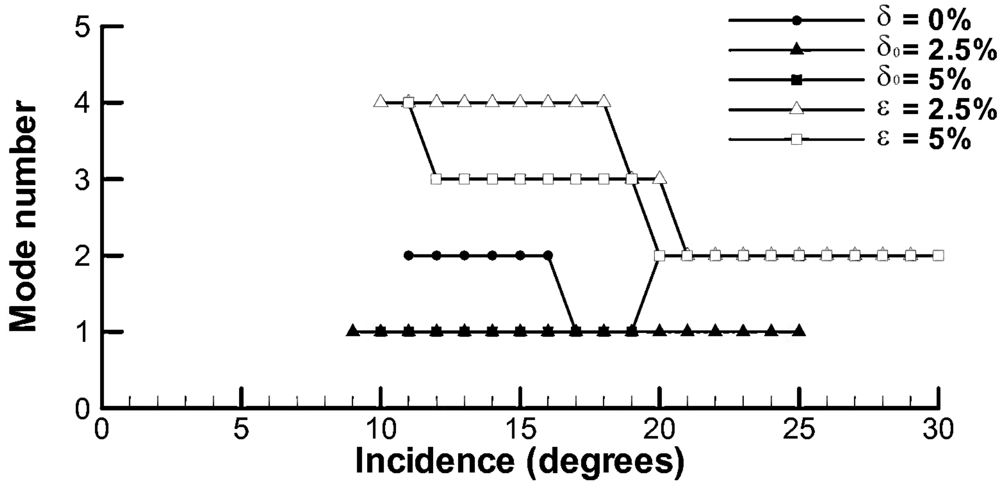

Figure 7: Variation of the mode number as a function of incidence for different wing's pre-strains and excess lengths for U_∞= 5 m/s.

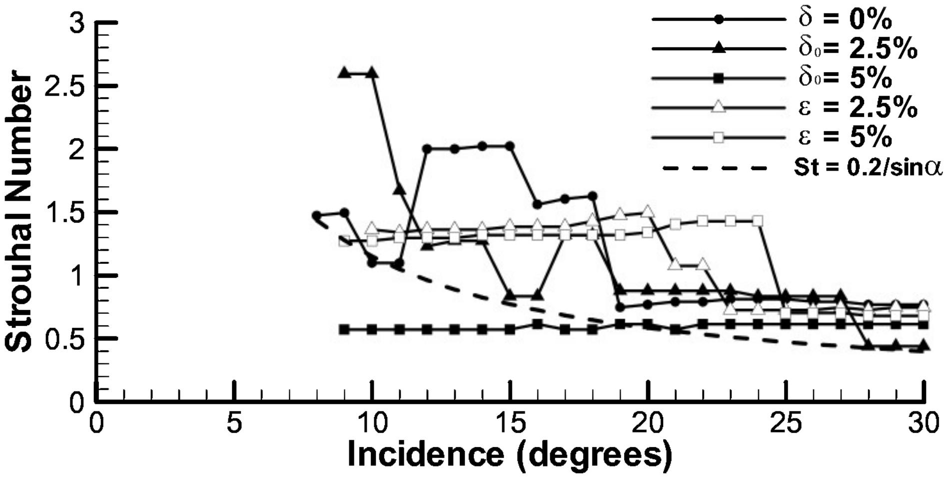

Figure 8: Variation of the Strouhal number of membrane oscillations as a function of incidence for different wing's pre-strains and excess lengths for U_∞= 10 m/s

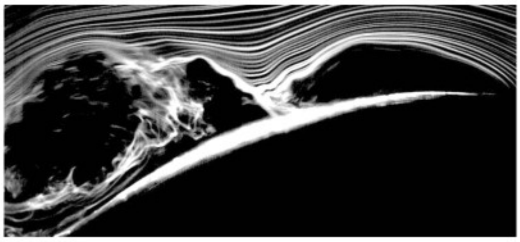

ε=2.5%

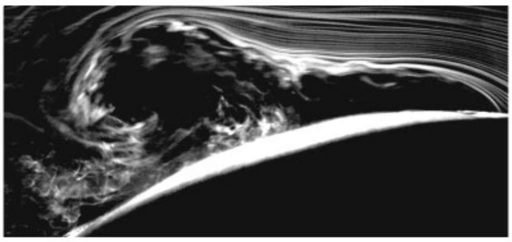

δ=0%

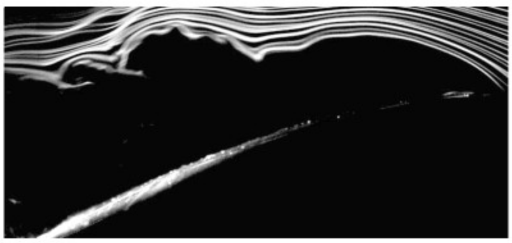

δ_0=2.5%

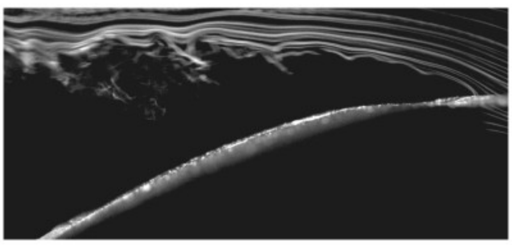

Rigid

Figure 9: Smoke flow visualization with a high speed camera for flexible (ε = 2.5%, δ = 0%, and δ_o = 2.5%) and rigid wings, U_∞= 5 m/s, α = 18°.

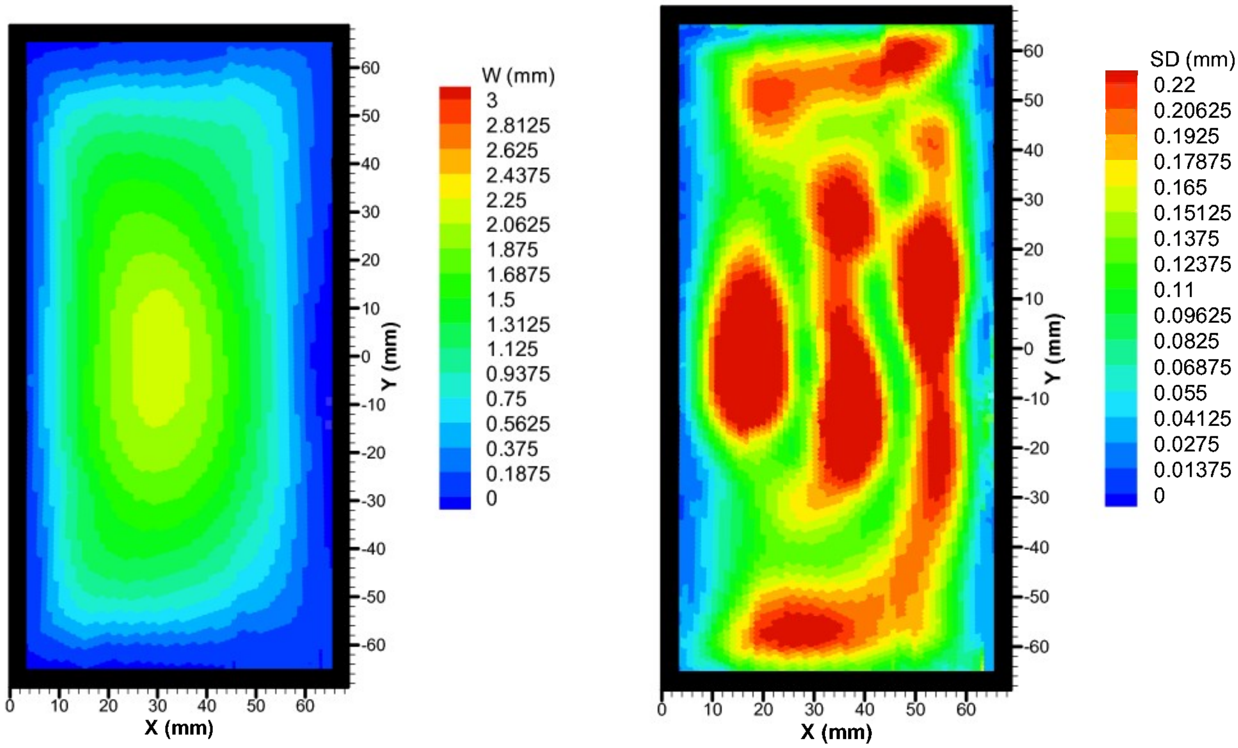

Figure 10: Mean and standard deviation of membrane deformation for a rectangular wing with aspect ratio AR=2, U_∞= 5 m/s, α = 10^o.